

Potentiodynamic and galvanostatic investigations of copper deposition from sulphate electrolytes containing large amount of zinc

G. A. Hodjaoglu, A. T. Hrussanova, I. S. Ivanov*

Institute of Physical Chemistry, Bulgarian Academy of Sciences, Acad. G. Bonchev St., Block 11, 1113 Sofia, Bulgaria

Received May 23, 2008; Revised February 25, 2009

The electroextraction of copper was studied on platinum cathode from sulphate electrolytes containing large amount of zinc. It was established that in electrolytes, containing $50 \text{ g}\cdot\text{dm}^{-3} \text{ Zn}^{2+}$ and 1 or $5 \text{ g}\cdot\text{dm}^{-3} \text{ Cu}^{2+}$ at potentials more negative than -1.6 V vs. SSE both copper and zinc deposition takes place. At concentration higher than $5 \text{ g}\cdot\text{dm}^{-3} \text{ Cu}^{2+}$ and in the presence of $130 \text{ g}\cdot\text{dm}^{-3} \text{ H}_2\text{SO}_4$ (independently of Cu^{2+} concentration) only copper is deposited. The addition of H_2SO_4 to the electrolyte leads to abrupt increase in cathodic current but it decreases the current efficiency of both copper and zinc deposition, which means that the current increase is a result of enhanced hydrogen evolution. The additive hydroxyethylated-2-butyne-1,4-diol (Ferasine) decreases the areas of Cu and Zn dissolution peaks, showing that the deposition process is inhibited. Dense, smooth and bright coatings of pure copper are deposited at current densities $0.5\text{--}2 \text{ A}\cdot\text{dm}^{-2}$ in electrolytes with Cu^{2+} concentration higher than $5 \text{ g}\cdot\text{dm}^{-3}$ in the presence of Ferasine. Non-adherent, dark-red slime of copper is obtained at lower Cu^{2+} concentrations.

Key words: copper, cyclic voltammograms, deposition, electroextraction, zinc.

INTRODUCTION

Metallurgy is a branch of the industry that affects very strongly the environment. After a number of pyro- or hydrometallurgical ores treating processes, large amount of wastes with high metal content remain. For example, the waste product known as “blue powder” that results by condensing furnace gases during the thermometallurgical processing of non-ferrous ores contains: Zn (25–41%), Pb (20–25%), Fe (3–5%), Cu (0.5–1%), Cd (0.5–1%), *etc.* [1, 2]. The purification of the electrolytes for Zn electrowinning by cementation is another process that produces wastes containing large amount of different metals such as: copper cake (containing 36–54% Cu, 5–10% Zn and 0.08–0.16% Cd), copper-cadmium cake (containing 10% Cu, 30% Zn, 12% Cd), collective cake (containing 5.8% Cu, 35.9% Zn, 7.2% Cd), copper-nickel cake (containing 25% Cu, 20% Zn, 3% Cd, 0.75% Co, 0.05% Ni). [3]. Cementates of the zinc industry, obtained during the hydrometallurgical zinc winning process, where the sulphate leach liquor is treated with arsenic trioxide and zinc powder for the removal of Cu, Ni, Co, Cd and other impurities before electrowinning, contain: Cu (28.6%), Zn (22.4%), Cd (6.7%), Co (1.32) and Ni (0.16%) [4]. Flue dusts in a secondary copper smelter treated in the electrowinning zinc plant contain: Zn (40–65%), Cu

(1–6%), (Pb 6–20%), Cd (0.5–0.8%), Ni (0.1–1%), Sn (1–2%), *etc.* [5]. Muresan *et al.* [2, 6] studied the process of Cu electrowinning from sulphate acidic electrolytes and observed that the addition of small amounts of Zn^{2+} had no effect on the composition of the Cu deposits, but it increased their microscopic roughness. The effect of horse-chestnut extract (HCE) and IT-85, representing a mixture of triethylbenzyl-ammonium chloride (TEBA) and hydroxyethylated-2-butyne-1,4-diol (Ferasine) upon the morphology and structure of Cu deposits was studied. The cathodic polarization was also investigated and compared to the effect exerted by thiourea and animal glue. The additive IT-85 was found to be an efficient inhibitor of the Cu electrocrystallization process, leading to levelled, fine-grained cathodic deposits. The effect of HCE was similar to the effect exerted by animal glue, leading to deposits consisting of rounded nodules, reflecting a smaller levelling effect. Varvara *et al.* [7–10] studied the influence of TEBA, Ferasine and IT-85 on the kinetics of Cu electrodeposition from such electrolytes and on the morphology and structure of Cu deposits. TEBA acts as an inhibitor of the electrodeposition process only as a blocking agent competing with cuprous ions for the adsorption sites of the cathodic surface. Due to its adsorption on the electrode surface, Ferasine inhibits the charge transfer and thus affects the electrocrystallization step, impeding the crystal growth process and promoting the nucleation of Cu. In spite of their different chemical nature, both additives were found

* To whom all correspondence should be sent:
E-mail: isivanov@ipc.bas.bg

to be efficient as levelling agents, leading to fine-grained cathodic deposits. Comparison of the inhibiting effects exerted by IT-85 and its components on the electrodeposition process pointed out to the existence of a beneficial complementarity of TEBA and Ferasine when they are used in mixture.

The aim of this paper was to study the influence of Zn^{2+} ions, Ferasine and some experimental conditions on the process of Cu electroextraction from sulphuric acid electrolytes.

EXPERIMENTAL

The experiments were carried out in a thermostated ($37 \pm 1^\circ C$), three-electrode glass cell without stirring of the electrolyte.

The cathode (2.0 cm^2) and both anodes (4.0 cm^2 total area), used in the potentiodynamic studies, were Pt plates. The reference electrode was a mercury/mercurous sulphate electrode in $0.5 \text{ M H}_2\text{SO}_4$ (SSE), its potential vs. NHE being $+0.720 \text{ V}$. The studies were carried out using a cyclic potentiodynamic technique. The potential scanning at a rate of $30 \text{ mV}\cdot\text{sec}^{-1}$ in the potential range from $+1.000$ to -1.800 V vs SSE was performed by means of computerized PAR 263A potentiostat/galvanostat using Soft Corr II software. The current efficiency of deposition process was obtained by integration of cathodic part and anodic peaks on the cyclic voltammograms (CV curves). The potential range and scanning rate were chosen experimentally as the most suitable.

Galvanostatic deposition was carried out using copper cathodes (4.0 cm^2) and two Pt anodes (4.0 cm^2 total area) at current densities in the range of $0.5\text{--}2 \text{ A}\cdot\text{dm}^{-2}$.

All electrodes were degreased in an ultrasound bath and then only Cu cathodes were etched in HNO_3 (1:1).

Cu^{2+} ions ($1, 5$ or $10 \text{ g}\cdot\text{dm}^{-3}$) were added to electrolytes, containing from 14 to $50 \text{ g}\cdot\text{dm}^{-3}$ Zn^{2+} ions (as $\text{ZnSO}_4\cdot 5\text{H}_2\text{O}$) and from 0 to $130 \text{ g}\cdot\text{dm}^{-3}$ H_2SO_4 . The organic additive was 30% solution of hydroxyethylated-butyne-2-diol-1,4 (Ferasine).

RESULTS AND DISCUSSION

Potentiodynamic studies

Influence of the vertex potential on CV curves.

Figure 1 shows CV curves obtained in an electrolyte, containing $50 \text{ g}\cdot\text{dm}^{-3}$ Zn^{2+} and $1 \text{ g}\cdot\text{dm}^{-3}$ Cu^{2+} . The potential scan direction is changed at cathodic potentials (vertex potentials) $-0.8, -1.2$ or -1.6 V . When the change of scan direction is made

at -0.8 or -1.2 V (curves 1 and 2) one little cathodic peak at -0.265 V and one higher cathodic peak at -0.455 V due to Cu deposition on the Pt surface are observed on the cathodic part of the curves. At more negative potentials simultaneous Cu deposition and hydrogen evolution is occurring. On the anodic part of each CV curve one high peak at -0.275 V (curve 1) and at -0.250 V (curve 2), due to the dissolution of the larger amount of the deposited Cu, and much lower one at 0.035 V (curve 1) and 0.130 V (curve 2), due to the dissolution of the Cu layer deposited on the Pt surface, are observed. When the vertex potential is -1.6 V (curve 3) on the cathodic part of the CV curve the two peaks due to Cu deposition are followed by sharp rise of the current due to codeposition of Cu and Zn as well as to hydrogen evolution. On the anodic part of the curve at -1.260 V peak of Zn dissolution appears, followed by the peaks of Cu dissolution at -0.210 V and 0.135 V , respectively. CV curves obtained in the presence of $1 \text{ cm}^3\cdot\text{dm}^{-3}$ of the organic additive Ferasine in the electrolyte are similar.

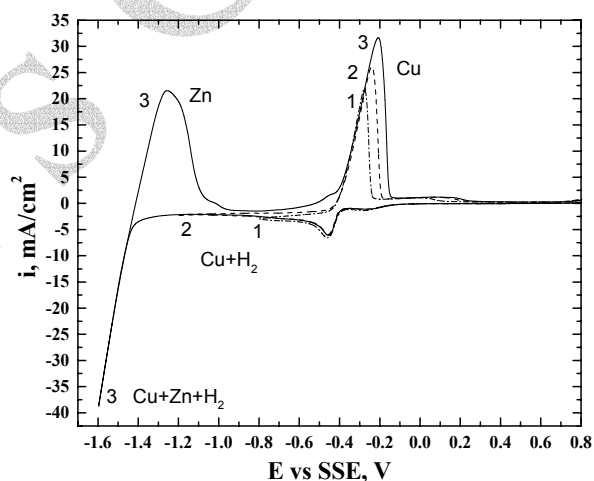


Fig. 1. Cyclic voltammograms, obtained on Pt cathode in an electrolyte, containing $50 \text{ g}\cdot\text{dm}^{-3}$ Zn^{2+} and $1 \text{ g}\cdot\text{dm}^{-3}$ Cu^{2+} . Vertex potentials vs. SSE (V): 1) -0.8 ; 2) -1.2 ; 3) -1.6 . Scan rate $30 \text{ mV}\cdot\text{sec}^{-1}$.

Figure 2 shows the CV curves obtained in an electrolyte, containing $50 \text{ g}\cdot\text{dm}^{-3}$ Zn^{2+} , $1 \text{ g}\cdot\text{dm}^{-3}$ Cu^{2+} and $130 \text{ g}\cdot\text{dm}^{-3}$ H_2SO_4 . The change of the scan direction is made at the same potentials as in the absence of acid. The peaks of Cu deposition are similar to those shown in Fig. 1. When the vertex potential is -1.6 V or more negative on the anodic part of the curves only peaks of Cu dissolution are observed. This shows that in the presence of H_2SO_4 Zn is not deposited. The addition of $1 \text{ cm}^3\cdot\text{dm}^{-3}$ Ferasine to the electrolyte does not change the CV curves.

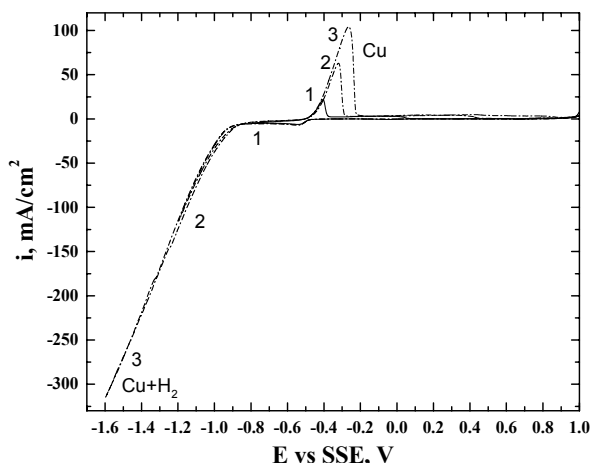


Fig. 2. Cyclic voltammograms, obtained on Pt cathode in an electrolyte, containing $50 \text{ g}\cdot\text{dm}^{-3} \text{ Zn}^{2+}$, $1 \text{ g}\cdot\text{dm}^{-3} \text{ Cu}^{2+}$ and $130 \text{ g}\cdot\text{dm}^{-3} \text{ H}_2\text{SO}_4$. Vertex potentials vs. SSE (V): 1) -0.8 ; 2) -1.2 ; 3) -1.6 . Scan rate $30 \text{ mV}\cdot\text{sec}^{-1}$.

CV curves obtained in an electrolyte, containing $50 \text{ g}\cdot\text{dm}^{-3} \text{ Zn}^{2+}$ and $10 \text{ g}\cdot\text{dm}^{-3} \text{ Cu}^{2+}$ are shown in Fig. 3. The change of the scan direction is made at the same potentials as in Figures 1 and 2. The cathodic part of the curves is similar to those obtained in the electrolyte, containing $1 \text{ g}\cdot\text{dm}^{-3} \text{ Cu}^{2+}$. The peaks of Cu deposition are higher, as it could be expected. Only peaks of Cu dissolution are observed on the anodic part of the curves showing that Zn deposition does not take place. The CV curves, obtained in the presence of Ferasine, H_2SO_4 or both H_2SO_4 and Ferasine are similar. In all cases Zn deposition does not take place, even if the vertex potential is -1.8 V .

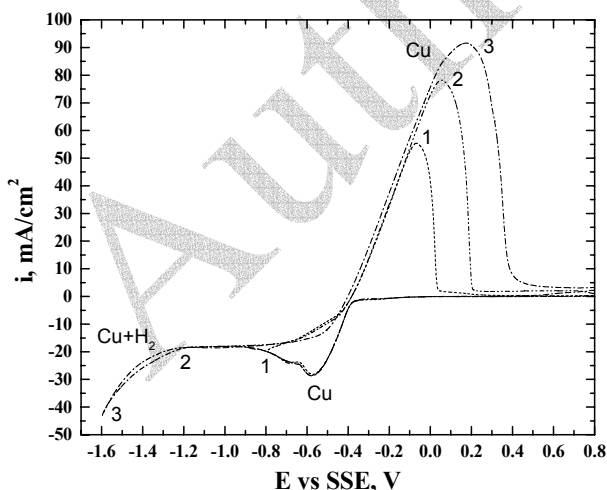


Fig. 3. Cyclic voltammograms, obtained on Pt cathode in an electrolyte, containing $50 \text{ g}\cdot\text{dm}^{-3} \text{ Zn}^{2+}$ and $10 \text{ g}\cdot\text{dm}^{-3} \text{ Cu}^{2+}$. Vertex potentials vs. SSE (V): 1) -0.8 ; 2) -1.2 ; 3) -1.6 . Scan rate $30 \text{ mV}\cdot\text{sec}^{-1}$.

Influence of the Cu^{2+} concentration and the vertex potential on the current efficiency of Cu and

Zn deposition. Integration of the cathodic part of CV curves as well as of the anodic peaks of Zn and Cu dissolution is used to determine the current efficiency of Zn and Cu deposition according to the following formulae:

$$CE_{\text{Zn}} [\%] = q_{\text{Zn}}^{\text{anode}} / q_{\text{Zn}}^{\text{cathode}} \cdot 100$$

$$CE_{\text{Cu}} [\%] = q_{\text{Cu}}^{\text{anode}} / q_{\text{Cu}}^{\text{cathode}} \cdot 100$$

Figure 4 shows the dependence of the current efficiency of Cu and Zn deposition on the vertex potential in electrolytes, containing $50 \text{ g}\cdot\text{dm}^{-3} \text{ Zn}^{2+}$ and $1, 5$ or $10 \text{ g}\cdot\text{dm}^{-3} \text{ Cu}^{2+}$, respectively. It can be seen that in the electrolyte, containing $1 \text{ g}\cdot\text{dm}^{-3} \text{ Cu}^{2+}$, when the change of scan direction is made at -1.4 V , the current efficiency of Cu deposition is $70\text{--}72\%$ and it decreases to about 20% , when the vertex potential is -1.8 V (curve 1a). In the same electrolyte the current efficiency of Zn deposition rises from 0% at vertex potential -1.4 V to about 75% at vertex potential -1.8 V (curve 1b). At Cu^{2+} concentration $5 \text{ g}\cdot\text{dm}^{-3}$ the current efficiency of Cu deposition is higher than 85% when the vertex potential is -1.6 V and it decreases to 75% at vertex potential -1.8 V (curve 2a). In the same electrolyte the current efficiency of Zn deposition rises from 0% at vertex potential -1.6 V to 15% at vertex potential -1.8 V (curve 2b). At Cu^{2+} concentration $10 \text{ g}\cdot\text{dm}^{-3}$ the current efficiency of Cu is in the range $80\text{--}95\%$ at all vertex potentials (curve 3). In this case, Zn is not deposited at all. The results obtained in electrolytes, containing Zn^{2+} $50 \text{ g}\cdot\text{dm}^{-3}$, Cu^{2+} ($1, 5$ or $10 \text{ g}\cdot\text{dm}^{-3}$) and $1 \text{ cm}^3\cdot\text{dm}^{-3}$ Ferasine are similar.

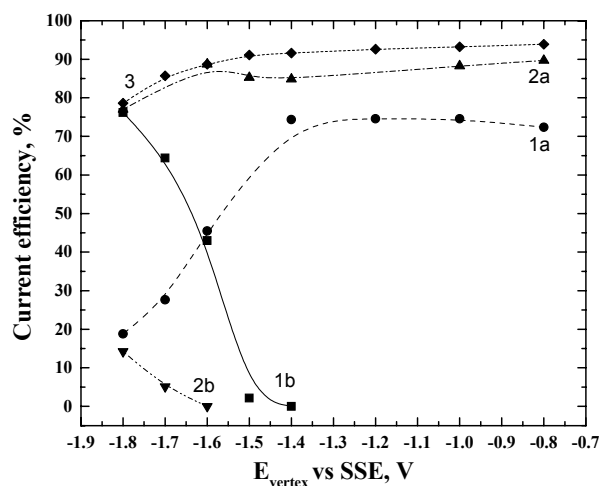


Fig. 4. Current efficiency (CE) of Cu and Zn deposition on Pt cathode vs. vertex potential (E_{vertex}). Electrolyte, containing $50 \text{ g}\cdot\text{dm}^{-3} \text{ Zn}^{2+}$ and $1 \text{ g}\cdot\text{dm}^{-3} \text{ Cu}^{2+}$; 1a) CE of Cu; 1b) CE of Zn. Electrolyte, containing $50 \text{ g}\cdot\text{dm}^{-3} \text{ Zn}^{2+}$ and $5 \text{ g}\cdot\text{dm}^{-3} \text{ Cu}^{2+}$; 2a) CE of Cu; 2b) CE of Zn. Electrolyte, containing $50 \text{ g}\cdot\text{dm}^{-3} \text{ Zn}^{2+}$ and $10 \text{ g}\cdot\text{dm}^{-3} \text{ Cu}^{2+}$; 3) CE of Cu.

In Figure 5 the dependence of current efficiency on vertex potential in electrolytes, containing $50 \text{ g}\cdot\text{dm}^{-3} \text{ Zn}^{2+}$, $130 \text{ g}\cdot\text{dm}^{-3} \text{ H}_2\text{SO}_4$ and 1, 5 or $10 \text{ g}\cdot\text{dm}^{-3} \text{ Cu}^{2+}$, respectively, is represented. The current efficiency of Cu decreases with the shift of vertex potential in negative direction, which is an indication of enhanced hydrogen evolution. As it could be expected, the increase in Cu^{2+} concentration leads to increase in the current efficiency. CV curves show that in the presence of H_2SO_4 at all Cu^{2+} concentrations Zn is not deposited. The addition of $1 \text{ cm}^3\cdot\text{dm}^{-3}$ Ferasine in these electrolytes does not lead to any significant changes in the CV curves.

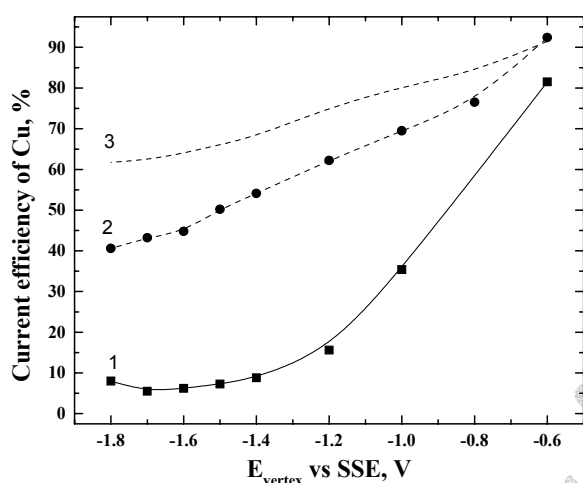


Fig. 5. Current efficiency (CE) of Cu deposition on Pt cathode vs. vertex potential (E_{vertex}). Electrolytes, containing $50 \text{ g}\cdot\text{dm}^{-3} \text{ Zn}^{2+}$, $130 \text{ g}\cdot\text{dm}^{-3} \text{ H}_2\text{SO}_4$ and: 1) $1 \text{ g}\cdot\text{dm}^{-3} \text{ Cu}^{2+}$; 2) $5 \text{ g}\cdot\text{dm}^{-3} \text{ Cu}^{2+}$; 3) $10 \text{ g}\cdot\text{dm}^{-3} \text{ Cu}^{2+}$.

Influence of H_2SO_4 and the organic additive Ferasine on the current efficiency of Cu and Zn deposition. Figure 6 shows the influence of the vertex potential on the current efficiency of Cu in electrolytes, containing $50 \text{ g}\cdot\text{dm}^{-3} \text{ Zn}^{2+}$ and 1 or $10 \text{ g}\cdot\text{dm}^{-3} \text{ Cu}^{2+}$ in presence or in absence of $130 \text{ g}\cdot\text{dm}^{-3} \text{ H}_2\text{SO}_4$. The current efficiency of Cu decreases in the presence of H_2SO_4 , (curves 2 and 4) compared to the current efficiency in absence of H_2SO_4 (curves 1a and 3). Zn is deposited in electrolytes containing $50 \text{ g}\cdot\text{dm}^{-3} \text{ Zn}^{2+}$ and only $1 \text{ g}\cdot\text{dm}^{-3} \text{ Cu}^{2+}$ (curve 1b).

The CV curves show that Ferasine decreases the cathodic current and the anodic peaks of metal deposition, which means that the organic additive inhibits the process. The influence of Ferasine is more pronounced in electrolytes without H_2SO_4 . The additive decreases the current efficiency of both metals, especially the current efficiency of Cu. In the presence of H_2SO_4 in the electrolyte Zn is not deposited at all vertex potentials.

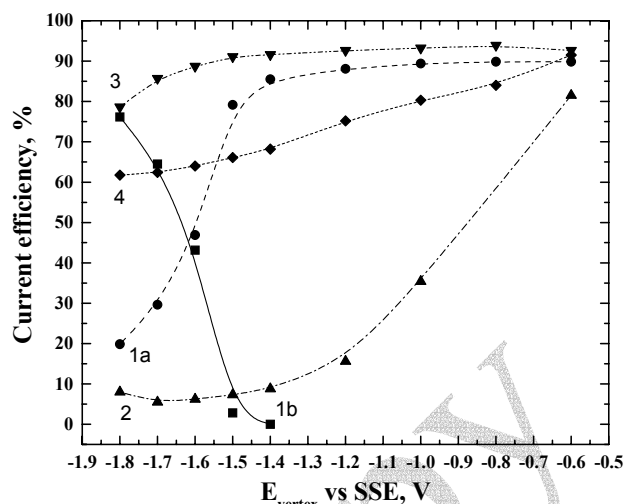


Fig. 6. Current efficiency (CE) of Cu and Zn deposition on Pt cathode versus vertex potential (E_{vertex}). Electrolyte, containing $50 \text{ g}\cdot\text{dm}^{-3} \text{ Zn}^{2+}$ and $1 \text{ g}\cdot\text{dm}^{-3} \text{ Cu}^{2+}$: 1a) CE of Cu; 1b) CE of Zn. Electrolyte, containing $50 \text{ g}\cdot\text{dm}^{-3} \text{ Zn}^{2+}$, $1 \text{ g}\cdot\text{dm}^{-3} \text{ Cu}^{2+}$ and $130 \text{ g}\cdot\text{dm}^{-3} \text{ H}_2\text{SO}_4$: 2) CE of Cu. Electrolyte, containing $50 \text{ g}\cdot\text{dm}^{-3} \text{ Zn}^{2+}$ and $10 \text{ g}\cdot\text{dm}^{-3} \text{ Cu}^{2+}$: 3) CE of Cu. Electrolyte, containing $50 \text{ g}\cdot\text{dm}^{-3} \text{ Zn}^{2+}$, $10 \text{ g}\cdot\text{dm}^{-3} \text{ Cu}^{2+}$ and $130 \text{ g}\cdot\text{dm}^{-3} \text{ H}_2\text{SO}_4$: 4) CE of Cu.

Galvanostatic studies

The effects of current density and electrolyte composition on the surface morphology and composition of galvanostatically deposited coatings on Cu substrates were also studied. In all cases only copper is detected by microprobe analysis.

It has been established that dense and smooth Cu coatings are deposited when the Cu^{2+} concentration is higher than $5 \text{ g}\cdot\text{dm}^{-3}$ and the current density is in the range $0.5 \div 2 \text{ A}\cdot\text{dm}^{-2}$. At density of $1 \text{ A}\cdot\text{dm}^{-2}$ the deposition potential is $-0.500 \div -0.600 \text{ V}$. In all cases the current efficiency of Cu deposition is higher than 95%. Figure 7 shows SEM micrograph of Cu coatings obtained after 3 h deposition at density of $1 \text{ A}\cdot\text{dm}^{-2}$ in an electrolyte, containing $50 \text{ g}\cdot\text{dm}^{-3} \text{ Zn}^{2+}$, $10 \text{ g}\cdot\text{dm}^{-3} \text{ Cu}^{2+}$ and $130 \text{ g}\cdot\text{dm}^{-3} \text{ H}_2\text{SO}_4$. The coating is light-red, smooth and semi-bright. The addition of Ferasine ($1 \text{ cm}^3\cdot\text{dm}^{-3}$) leads to more fine-grained surface morphology of the coatings (Fig. 8). The additive effect is more strongly expressed at Ferasine concentration $5 \text{ cm}^3\cdot\text{dm}^{-3}$. In the presence of Ferasine the coatings are light-red, smooth and bright. Coatings obtained in electrolytes containing $20 \text{ g}\cdot\text{dm}^{-3} \text{ Cu}^{2+}$ and, respectively 50 and $100 \text{ g}\cdot\text{dm}^{-3} \text{ Zn}^{2+}$ are more coarse-grained but in the first case they are bright, while in the second – dark-red and rough.

The grain size of all coatings is presented in Table 1.

Table 1. Grain size of Cu coatings obtained in different electrolytes (in μm).

Electrolyte	Grain size, μm
$50 \text{ g}\cdot\text{dm}^{-3} \text{ Zn}^{2+} + 10 \text{ g}\cdot\text{dm}^{-3} \text{ Cu}^{2+}$	25–30
$50 \text{ g}\cdot\text{dm}^{-3} \text{ Zn}^{2+} + 10 \text{ g}\cdot\text{dm}^{-3} \text{ Cu}^{2+} + 1 \text{ ml}\cdot\text{dm}^{-3} \text{ Ferasine}$	15–18
$50 \text{ g}\cdot\text{dm}^{-3} \text{ Zn}^{2+} + 10 \text{ g}\cdot\text{dm}^{-3} \text{ Cu}^{2+} + 130 \text{ g}\cdot\text{dm}^{-3} \text{ H}_2\text{SO}_4$	12–18
$50 \text{ g}\cdot\text{dm}^{-3} \text{ Zn}^{2+} + 10 \text{ g}\cdot\text{dm}^{-3} \text{ Cu}^{2+} + 130 \text{ g}\cdot\text{dm}^{-3} \text{ H}_2\text{SO}_4 + 1 \text{ cm}^3\cdot\text{dm}^{-3} \text{ Ferasine}$	10–12
$50 \text{ g}\cdot\text{dm}^{-3} \text{ Zn}^{2+} + 10 \text{ g}\cdot\text{dm}^{-3} \text{ Cu}^{2+} + 130 \text{ g}\cdot\text{dm}^{-3} \text{ H}_2\text{SO}_4 + 5 \text{ cm}^3\cdot\text{dm}^{-3} \text{ Ferasine}$	< 3
$50 \text{ g}\cdot\text{dm}^{-3} \text{ Zn}^{2+} + 20 \text{ g}\cdot\text{dm}^{-3} \text{ Cu}^{2+} + 130 \text{ g}\cdot\text{dm}^{-3} \text{ H}_2\text{SO}_4 + 5 \text{ cm}^3\cdot\text{dm}^{-3} \text{ Ferasine}$	9–12
$100 \text{ g}\cdot\text{dm}^{-3} \text{ Zn}^{2+} + 20 \text{ g}\cdot\text{dm}^{-3} \text{ Cu}^{2+} + 130 \text{ g}\cdot\text{dm}^{-3} \text{ H}_2\text{SO}_4 + 5 \text{ cm}^3\cdot\text{dm}^{-3} \text{ Ferasine}$	15–20
$50 \text{ g}\cdot\text{dm}^{-3} \text{ Zn}^{2+} + 5 \text{ g}\cdot\text{dm}^{-3} \text{ Cu}^{2+} + 130 \text{ g}\cdot\text{dm}^{-3} \text{ H}_2\text{SO}_4 + 5 \text{ cm}^3\cdot\text{dm}^{-3} \text{ Ferasine}$	< 6
$14 \text{ g}\cdot\text{dm}^{-3} \text{ Zn}^{2+} + 1.25 \text{ g}\cdot\text{dm}^{-3} \text{ Cu}^{2+} + 16.5 \text{ g}\cdot\text{dm}^{-3} \text{ H}_2\text{SO}_4 + 0.6 \text{ cm}^3\cdot\text{dm}^{-3} \text{ Ferasine}$	< 1–2

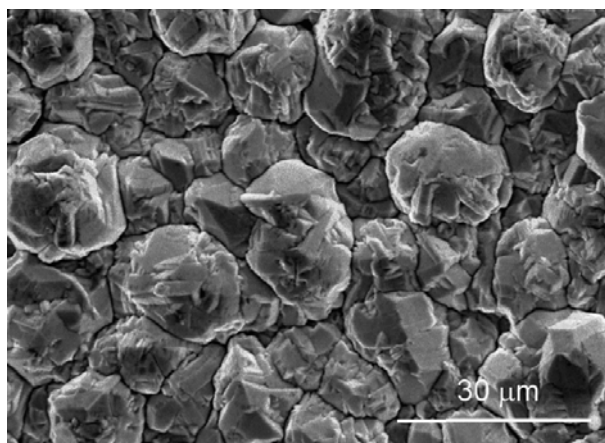


Fig. 7. SEM micrograph of Cu coating, obtained after 3 h deposition at density $1 \text{ A}\cdot\text{dm}^{-2}$ in an electrolyte, containing $50 \text{ g}\cdot\text{dm}^{-3} \text{ Zn}^{2+}$, $10 \text{ g}\cdot\text{dm}^{-3} \text{ Cu}^{2+}$ and $130 \text{ g}\cdot\text{dm}^{-3} \text{ H}_2\text{SO}_4$. Magnification $\times 1000$.

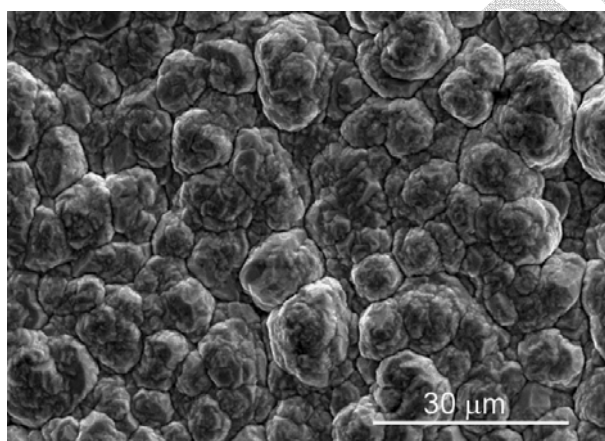


Fig. 8. SEM micrograph of Cu coating, obtained after 2 h deposition at density $1 \text{ A}\cdot\text{dm}^{-2}$ in an electrolyte, containing $50 \text{ g}\cdot\text{dm}^{-3} \text{ Zn}^{2+}$, $10 \text{ g}\cdot\text{dm}^{-3} \text{ Cu}^{2+}$, $130 \text{ g}\cdot\text{dm}^{-3} \text{ H}_2\text{SO}_4$ and $1 \text{ cm}^3\cdot\text{dm}^{-3} \text{ Ferasine}$. Magnification $\times 1000$.

It was established that non-adherent, dark-red Cu slime is deposited on Cu substrate at Cu^{2+} concentration lower than $5 \text{ g}\cdot\text{dm}^{-3}$. In the case of low Cu^{2+} concentration the deposition potential is more negative (between -1.000 and -1.100 V) due to the concentration polarization. Figure 9 shows the morphology of Cu slime obtained after 30 min

deposition at density $0.5 \text{ A}\cdot\text{dm}^{-2}$ and potential -1.05 V in an electrolyte, containing $1.25 \text{ g}\cdot\text{dm}^{-3} \text{ Cu}^{2+}$, $14 \text{ g}\cdot\text{dm}^{-3} \text{ Zn}^{2+}$, $16.5 \text{ g}\cdot\text{dm}^{-3} \text{ H}_2\text{SO}_4$ and $0.6 \text{ cm}^3\cdot\text{dm}^{-3}$ Ferasine. In this case the current efficiency is less than 75%.

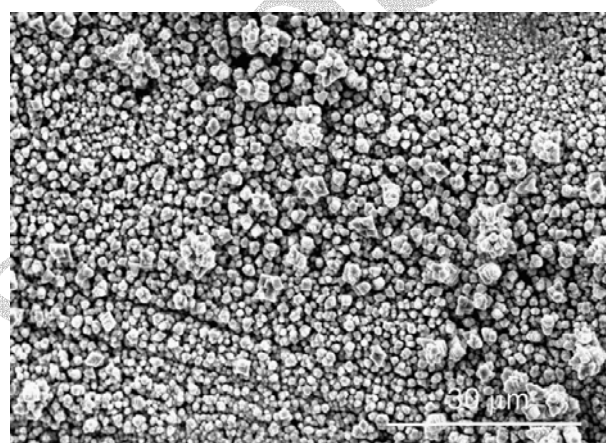


Fig. 9. SEM micrograph of Cu coating, obtained after 30 min deposition at density $0.5 \text{ A}\cdot\text{dm}^{-2}$ in an electrolyte, containing $14 \text{ g}\cdot\text{dm}^{-3} \text{ Zn}^{2+}$, $1.25 \text{ g}\cdot\text{dm}^{-3} \text{ Cu}^{2+}$, $16.5 \text{ g}\cdot\text{dm}^{-3} \text{ H}_2\text{SO}_4$ and $0.6 \text{ cm}^3\cdot\text{dm}^{-3} \text{ Ferasine}$. Magnification $\times 1000$.

CONCLUSIONS

In electrolytes, containing $50 \text{ g}\cdot\text{dm}^{-3} \text{ Zn}^{2+}$ and 1 or $5 \text{ g}\cdot\text{dm}^{-3} \text{ Cu}^{2+}$ at potentials more negative than -1.6 V vs. SSE simultaneous deposition of Cu and Zn on Pt cathode is taking place. With the increase in Cu^{2+} concentration, the anodic peaks of Zn dissolution decrease. At Cu^{2+} concentration $10 \text{ g}\cdot\text{dm}^{-3}$ only Cu deposition takes place. In electrolytes, containing $50 \text{ g}\cdot\text{dm}^{-3} \text{ Zn}^{2+}$ and $130 \text{ g}\cdot\text{dm}^{-3} \text{ H}_2\text{SO}_4$ at all studied Cu^{2+} concentrations and vertex potentials only Cu deposition takes place.

In electrolytes, containing $50 \text{ g}\cdot\text{dm}^{-3} \text{ Zn}^{2+}$ current efficiency of Cu deposition at vertex potentials more negative than -1.6 V vs. SSE decreases from 70% to 20% (at Cu^{2+} concentration $1 \text{ g}\cdot\text{dm}^{-3}$) and from 85–90% to 75–80% (at Cu^{2+} concentration 5 or $10 \text{ g}\cdot\text{dm}^{-3}$). As it is expected current efficiency of Cu increases with the increase in Cu^{2+} concentration. Current efficiency of Zn deposition increases at

vertex potentials more negative than -1.6 V vs. SSE from 0 to 75% and 15% (at Cu^{2+} concentrations of 1 and $5 \text{ g}\cdot\text{dm}^{-3}$, respectively). At Cu^{2+} concentration of $10 \text{ g}\cdot\text{dm}^{-3}$ Zn deposition does not take place.

In electrolytes containing $50 \text{ g}\cdot\text{dm}^{-3} \text{ Zn}^{2+}$ and $130 \text{ g}\cdot\text{dm}^{-3} \text{ H}_2\text{SO}_4$ the current efficiency of Cu deposition increases with the increase in Cu^{2+} concentration and decreases with the increase in the vertex potential. In all cases Zn deposition does not take place. The current efficiency of Cu deposition in the presence of $130 \text{ g}\cdot\text{dm}^{-3} \text{ H}_2\text{SO}_4$ is lower than the current efficiency in its absence.

Dense and smooth copper coatings on Cu cathode with current efficiency higher than 95% are deposited when Cu^{2+} concentration is higher than $5 \text{ g}\cdot\text{dm}^{-3}$ and the current density is in the range $0.5\text{--}2 \text{ A}\cdot\text{dm}^{-2}$. More fine-grained coatings are obtained in the presence of H_2SO_4 and the organic additive hydroxyethylated-2-butyne-1,4-diol (Ferasine). At lower Cu^{2+} concentration, non-adherent dark-red slime of copper is deposited with current efficiency less than 75%.

REFERENCES

1. L. Muresan, A. Nicoara, S. Varvara, G. Maurin, *J. Appl. Electrochem.*, **29**, 719 (1999).
2. L. Muresan, S. Varvara, G. Maurin, S. Dorneanu, *Hydrometallurgy*, **54**, 161 (2000).
3. V. D. Karoleva, *Metallurgy of Heavy Non-ferrous Metals, Part II*, c/o Jusautor, Sofia, 1986.
4. D. Melzner, J. Tilkowski, A. Mohrmann, W. Poppe, W. Halwachs, K. Schogerl, *Hydrometallurgy*, **13**, 105 (1984).
5. R. Kammel, M. Goktepe, H. Oelmann, *Hydrometallurgy*, **19**, 11 (1987).
6. L. Muresan, A. Nicoara, S. Varvara, G. Maurin, *J. Appl. Electrochem.*, **29**, 719 (1999).
7. S. Varvara, L. Muresan, I. C. Popescu, G. Maurin, *J. Appl. Electrochem.*, **33**, 685 (2003).
8. S. Varvara, L. Muresan, I. C. Popescu, G. Maurin, *Hydrometallurgy*, **75**, 147 (2004).
9. S. Varvara, L. Muresan, A. Nicoara, G. Maurin, I. C. Popescu, *Mater. Chem. Phys.* **72**, 332 (2001).
10. S. Varvara, L. Muresan, I. C. Popescu, G. Maurin, *J. Appl. Electrochem.* **35**, 69 (2005).

ПОТЕНЦИОДИНАМИЧНИ И ГАЛВАНСТАТИЧНИ ИЗСЛЕДВАНИЯ НА ОТЛАГАНЕ НА МЕД ОТ СУЛФАТНИ ЕЛЕКТРОЛИТИ СЪДЪРЖАЩИ ГОЛЕМИ КОЛИЧЕСТВА ЦИНК

Г. А. Ходжаоглу, А. Т. Хрусанова, И. С. Иванов*

Институт по физикохимия, Българска академия на науките, ул. „Акад. Г. Бончев“, бл. 11, 1113 София

Постъпила на 23 май 2008 г.; Преработена на 25 февруари 2009 г.

(Резюме)

Изследвана е електроекстракцията на мед върху платинов катод от сулфатни електролити, съдържащи големи количества цинк. Установено е, че в електролити, съдържащи $50 \text{ g}\cdot\text{dm}^{-3} \text{ Zn}^{2+}$ и 1 или $5 \text{ g}\cdot\text{dm}^{-3} \text{ Cu}^{2+}$, при потенциали по-отрицателни от -1.6 V vs. SSE се отлагат едновременно мед и цинк. При концентрация на Cu^{2+} по-висока от $5 \text{ g}\cdot\text{dm}^{-3}$ и в присъствие на $130 \text{ g}\cdot\text{dm}^{-3} \text{ H}_2\text{SO}_4$ (независимо от концентрацията на Cu^{2+}) се отлага само мед. Прибавянето към електролита на H_2SO_4 води до рязко нарастване на катодния ток, но същевременно понижава добива по ток, както на отлагането на мед, така и на цинк, което означава, че нарастването на тока е резултат от засиленото отделяне на водород. Добавката хидроксиетилиран-2-бутин-1,4-диол (Ферасин) намалява площта на медните и цинкови пикове на разтваряне, което показва, че процесът на отлагане е инхибиран. Плътни, гладки и блестящи покрития от чиста мед се отлагат при плътности на тока $0.5\text{--}2 \text{ A}\cdot\text{dm}^{-2}$ в електролити с концентрации на Cu^{2+} по-високи от $5 \text{ g}\cdot\text{dm}^{-3}$ в присъствие на Ферасин. Тъмночервен и със слаба адхезия към катода меден шлам се получава при по-ниски концентрации на Cu^{2+} .